

Connecting polymers to the quantum Hall plateau transition

Joel E. Moore

Bell Labs Lucent Technologies, 600 Mountain Avenue, Murray Hill, NJ 07974

(December 2, 2024)

A mapping is developed between the quantum Hall plateau transition and the statistics of self-interacting lattice polymers. This mapping is exact in the classical percolation limit of the plateau transition, and diffusive behavior at the critical energy is shown to be related to the critical exponents of a class of chiral polymers at the θ -point. The exact critical exponents of the chiral polymer model on the honeycomb lattice are found, verifying that this model is in the same universality class as a previously solved model of polymers on the Manhattan lattice. The mapping is obtained by averaging analytically over the local random potentials in a previously studied lattice model for the classical plateau transition. This average generates a weight on chiral polymers associated with the classical localization length exponent $\nu = 4/3$. We argue that quantum effects should be more accessible in the polymer formulation than in the customary percolation language, and discuss a possible relationship between the quantum transition and nonchiral polymers at θ . Some properties of the polymer models are verified by transfer matrix and Monte Carlo studies.

PACS numbers: 73.43.Nq, 72.15.Rn, 61.41.+e

I. INTRODUCTION

The quantum Hall plateau transition is of great interest because it links Anderson localization and the quantum Hall effect (QHE), two of the fundamental phenomena of condensed matter physics. Noninteracting electrons moving in two dimensions in a random potential form energy eigenstates which do not extend to infinity but are exponentially localized in finite regions of the plane. The situation changes drastically in a magnetic field: there are then extended states at discrete critical energies E_c separated by the cyclotron energy $\hbar\omega_c$. These extended states are remnants of the Landau bands at zero disorder. At other energies the electron eigenstates are localized, and the localization length near a critical energy scales according to

$$\xi(E) = \xi_0 \left(\frac{E_c}{E - E_c} \right)^\nu. \quad (1.1)$$

An understanding of this behavior, which determines the passage from one quantum Hall plateau to another, is essential to the explanation of the integer QHE¹. Despite progress in finding an effective theory for this transition^{2,3}, the scaling law (1.1) and other universal properties of the transition have still not been obtained analytically.

The clearest picture for the scaling (1.1) remains the connection between hulls of percolation clusters and classical electron trajectories in a strong magnetic field and random potential⁴. Classical percolation was recently shown to describe correctly some aspects of the *spin* quantum Hall transition⁵, but the ordinary quantum Hall transition is known from numerical studies^{6,7} not to lie in the percolation universality class. Considerable effort has been devoted to how quantum effects modify the percolation picture, and while there is now an understanding via numerics of the essential ingredients required to

model the transition⁷, analytic progress on generalizing percolation has been quite limited⁸. This paper develops a mapping between the plateau transition and the physics of self-interacting two-dimensional lattice polymers. Many statistical properties are known for such polymers because they in turn can be mapped to simple magnetic systems with known critical properties^{9,10}. A major motivation for the polymer mapping is that a simple argument suggests that quantum effects only change the weights assigned to different polymers. Hence polymers may provide a better classical starting point than percolation for understanding the quantum transition.

The properties of a lattice version of the classical plateau transition are mapped after disorder averaging onto polymers at the θ -point, which is a tricritical point separating the collapsed and extended phases of polymers with an attractive short-ranged self-interaction. The polymer model for the classical transition gives a useful complementary picture to the percolation description, in which some facts, such as diffusion at the critical energy, are more easily recovered. A side benefit is that some new results on polymers come out naturally from the mapping to the plateau transition.

The polymer mapping provides an alternate connection between the classical limit of the plateau transition and (classical) percolation^{4,11,12}, as ring polymers at the θ -point are equivalent to percolation hulls^{13,14}. One result of this paper is that directly mapping the plateau transition to polymers without the intermediate step of percolation gives many more relations. The exponent ν_θ which governs the typical size of a polymer (for a polymer of N units, $\langle R^2 \rangle \sim N^{2\nu_\theta}$, where $\langle \rangle$ denote averages over the ensemble of polymers), and μ and γ which determine essentially the number $\sim \mu^N N^{\gamma-1}$ of polymers of length N , can all be connected to the plateau transition.

The localization length exponent in (1.1) is $\nu = \frac{4}{3}$ for classical percolation, while numerical studies^{6,7} for the

quantum case predict $\nu = 2.35 \pm 0.05$ for the lowest Landau level (LLL), consistent with experiments¹⁵. In this paper ν will be studied via the subdiffusive propagation of electrons in a magnetic field and quenched random potential, which is now reviewed. Recently it was shown by Sinova, Meden, and Girvin¹⁶ that the localization length exponent ν appears in the energy-integrated correlation function $\Pi(x, t) \equiv \langle\langle \bar{\rho}(0, 0) \bar{\rho}(x, t) \rangle\rangle$, where $\bar{\rho}$ is the LLL-projected electron density operator and $\langle\langle \rangle\rangle$ denote disorder averaging. (The discussion in this paper is generally restricted to the LLL, although ν is believed to be universal.) The Fourier transform was verified numerically to have the scaling form

$$\omega \text{Im} \Pi(q, \omega) = \omega^{\frac{1}{2\nu}} f(q^2/\omega) \quad (1.2)$$

in the limit $q, \omega \rightarrow 0$ with $q^2 \ll \omega$. This scaling form can be understood as resulting from a simple form for $\Pi(q, \omega)$ in this limit,

$$\Pi(q, \omega) \sim \frac{1}{\omega - iD(\omega)q^2}, \quad (1.3)$$

with the frequency-dependent diffusion constant $D(\omega) \propto \omega^{\frac{1}{2\nu}}$.

The result (1.2) depends on the assumption that only at isolated critical energies E_c are there extended states. It can be understood from the following argument, which is somewhat different from that in¹⁶. Electrons at energy E with localization length $\xi(E)$ move diffusively over short times but cross over to localized behavior once $t \geq \xi(E)^2/D_0$. The diffusion constant D_0 should have a finite limit as $E \rightarrow E_c$ since the conductivity σ_{xx} is finite at the transition, and can be approximated by this limiting value in the scaling limit. So for a particle at the origin at $t = 0$ (where it projects onto eigenstates of different energies),

$$\langle x^2(t) \rangle \approx \int_{\xi(E)=\sqrt{D_0 t}}^{\infty} dE \rho \xi^2(E) + \int_{E_c}^{\xi(E)=\sqrt{D_0 t}} dE \rho D_0 t. \quad (1.4)$$

where ρ is the density of states near E_c . This results in subdiffusive behavior:

$$\tilde{D} \equiv \frac{d}{dt} \langle x^2(t) \rangle = 2D_0(\rho E_c) \left(\frac{\xi_0}{\sqrt{D_0}} \right)^{\frac{1}{\nu}} t^{-\frac{1}{2\nu}}, \quad (1.5)$$

which corresponds to (1.2) with $f(x) \propto x$ for $x \ll 1$.

Our starting point to obtain the anomalous diffusion (1.2) is a single electron moving either classically or quantum-mechanically in the x - y plane in a random potential $V(x)$ and strong constant magnetic field $B\hat{z}$. The classical coarse-grained equation of motion

$$B\dot{\mathbf{x}}_i = -\epsilon_{ij} \partial_j V(x) \quad (1.6)$$

can also be obtained¹² by taking a certain limit of the Liouvillian formalism. The lowest-Landau-level projected

electron density operator in this limit becomes a classical distribution function of particles moving according to (1.6). Of course, the equation of motion (1.6) can also be derived simply from classical physics: a single electron moving in constant electric and magnetic fields with $E < B$ has average velocity $\frac{E}{B}c$ along the direction $\mathbf{E} \times \mathbf{B}$. Since the direction of motion is always perpendicular to ∇V , the particle moves along a constant-energy contour of the potential. The picture underlying network models⁷ of the transition is that electron propagation is nearly classical except near a saddle point of the potential, where quantum tunneling becomes significant.

The first part of this paper shows that a discrete-time lattice version of (1.6), known to have the correct (percolative) critical scaling for the classical limit, maps after disorder averaging onto a model of two-dimensional interacting polymers on the same lattice. Although the lattice is useful to derive the mapping, the critical properties related by the mapping are universal and hence lattice-independent. The second part of this paper argues that the full quantum-mechanical plateau transition should be described in principle by some other polymer model, and considers several examples. In the remainder of the introduction, we outline the lattice model of (1.6) and some basic properties of interacting polymers, then summarize the main results.

In order to establish the connection between polymers and motion along level surfaces, we use a lattice model due to Gurarie and Zee¹². The particle is taken to have constant velocity along level surfaces: a nonzero mean velocity at criticality was found numerically in^{11,12} for similar models, and fixing the particle velocity does not alter the critical scaling. Particles move on the edges of the honeycomb lattice of Fig. 1, where each hexagonal face has an associated random potential energy. Except in section II, the energy E of a particle starting at vertex A will be taken to be the average of the three neighboring potentials V_1, V_2, V_3 , instead of an independent quantity as in¹². The energy E is constant along the particle trajectory. The particle's first step is chosen so that the largest of V_1, V_2, V_3 lies to the left. In successive steps, there is always a choice between two directions aside from the direction by which the particle entered, and only one of these choices will satisfy the condition that the energy to the left (right) be greater (less) than E . For each realization of the random potentials and each starting point, there is a unique locus of the particle after N steps. The connection to the classical localization exponent $\nu = \frac{4}{3}$ is that the mean square displacement after N steps is found to show subdiffusive behavior:

$$\langle\langle R^2(N) \rangle\rangle \sim N^{1-\frac{1}{2\nu}} \quad (1.7)$$

in accord with (1.5). The value $1 - \frac{1}{2\nu} \approx 0.62$ was found by numerical simulation¹² of (1.6), compared to the predicted value $\frac{5}{8} = 0.625$.

Now the connection between motion along level surfaces (1.6) and percolation hulls is quickly reviewed. Consider the level-surface motion on the hexagonal lattice

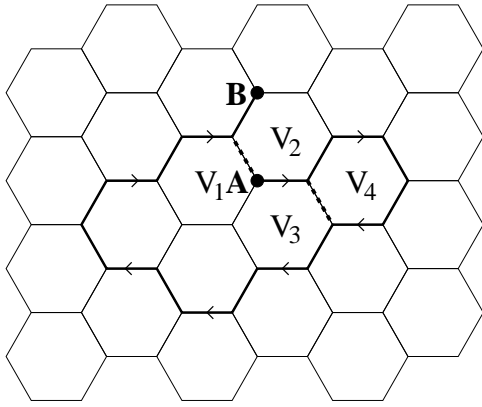


FIG. 1. Sample self-avoiding walk from A to B of 20 steps, with 19 neighboring hexagons. The dotted edges are self-contacts: the edge between V_3 and V_4 is an antiparallel self-contact, while that between V_1 and V_2 is a parallel self-contact. This path is not allowed classically since the walk passes V_2 both on the left and on the right.

with white-noise potentials (i.e., the disorder correlation length λ_D is less than the lattice spacing). Then all potentials on the left of a trajectory are higher than the trajectory energy E , which is higher than all potentials on the right. Now let all faces with energy higher than E be “colored”, while those with energy lower than E remain uncolored. The trajectory is then a hull separating colored faces from uncolored ones, and the properties of such hulls are a standard problem in percolation. Although the choice of lattice affects such properties as the density of colored faces at the critical point, critical exponents are universal (independent of the lattice). Similarly a lattice model is used here to establish the mapping to a polymer problem, but the universal polymer properties γ and ν discussed below do not depend on this lattice.

The usual way to study this type of lattice model^{11,12} is by summing numerically over paths at fixed particle energy. Here the path will be held fixed for the integration over random potentials: the goal is to assign a weight to each path according to the fraction of the space of random potentials for which that path is the particle trajectory. For convenience, the potentials are assumed to be uniformly distributed on $[-1, 1]$, so the critical energy is $E_0 = 0$. After N steps the particle has either moved along a self-avoiding walk (SAW) of length N , or else has looped and begun retracing previous steps. There is a constraint of “no parallel self-contacts” (the terminology is explained in section II) on allowed SAWs resulting from the restriction that no hexagon can be passed on both the left and right (Fig. 1).

The probability $P(a, b, N)$ to reach b from a after N steps can be written as a sum over an ensemble of paths including both closed self-avoiding polygons (SAPs) as well as open SAWs with no parallel self-contacts. Writing W^i for the weight of closed or open curve i , the disorder-averaged probability to be at b after N steps starting

from a is (H is the number of different hexagons visited by the SAW or SAP)

$$P(a, b, N) \propto \sum_{\substack{\text{SAPs } i \text{ through } a \text{ and } b, \\ l = \text{length of SAP}, \\ q = \text{steps from } a \text{ to } b}} \delta_{N \bmod l, q} W^i + \sum_{\substack{\text{SAWs } j \text{ of length } N \\ \text{from } a \text{ to } b \\ \text{no } \parallel \text{ self-contacts}}} W^j. \quad (1.8)$$

In the above each SAP should actually be summed twice, once with distance q and once with distance $l - q$. The δ -function in the SAW part ensures that the particle location after N steps is b . Sections II and III carry out the disorder average to calculate the weights $W^{i,j}$ exactly for cases of interest. The weights turn out to have a natural interpretation in terms of self-interacting polymers.

In section II we demonstrate that the trajectories of the lattice model at the critical energy E are related to a chiral polymer model, whose exact critical properties are found. The property of diffusion at the critical energy is shown to follow from the critical exponents $\gamma = \frac{6}{7}$ and $\nu_\theta = \frac{4}{7}$ of the polymer problem. Then in section III we modify the model so that the energy of a trajectory is a function of initial position rather than an independent quantity, and study the localization exponent ν . An inequality is derived which connects ν to the exponents of the associated polymer problem. Finally, in section IV we discuss the modifications to the polymer picture resulting from the inclusion of quantum-mechanical tunneling. Two polymer ensembles are examined for possible relevance to the quantum plateau transition.

II. TRAJECTORIES AT THE CRITICAL ENERGY

At the critical energy, the particle motion is diffusive: $\langle\langle R^2(N) \rangle\rangle \sim N$ for long times N . This section shows that the conditional probability $P(a, b, N, E_0)$ for the particle moves from a to b after N steps, given that the particle energy is the critical energy E_0 , is related to critical properties of self-interacting polymers at the θ -point. Then in the following section the same mapping will be shown to give information about trajectories at other energies, and hence about ν . We note in passing that in the percolation picture, diffusion at the critical energy is somewhat surprising. A particle on the hull of the infinite cluster moves superdiffusively, while a particle on a finite cluster has only bounded motion: the diffusive motion obtained after averaging over initial position essentially interpolates between these two limits.

For a path P_{AB} at the critical energy E_0 , the probability that P_{AB} is the trajectory in a random potential realization is proportional to $2^{-H_L} 2^{-H_R} = 2^{-H}$. Here H_L (H_R) is the number of hexagons passed on the left (right) by the path, and $H = H_L + H_R$: the probability

2^{-H} comes about because each hexagon i with potential V_i is as likely to have $V_i > E_0$ as to have $V_i < E_0$. Then the ensemble (1.8) becomes

$$P(a, b, N, E_0) = \sum_{\substack{\text{SAPs through } a \text{ and } b, \\ l = \text{length of SAP}, \\ q = \text{steps from } a \text{ to } b}} \frac{\delta_{N \bmod l, q}}{2^H} + \sum_{\substack{\text{SAWs of length } N \\ \text{from } a \text{ to } b \\ \text{no } \parallel \text{ self-contacts}}} \frac{1}{2^H}. \quad (2.1)$$

The connection to self-interacting polymers appears because the number of hexagons visited by an SAW is related to the number of self-contacts of the SAW. A self-contact is a point where the SAW is within one edge of intersecting itself. Counting hexagons in lieu of self-contacts gives rise to the famous θ' model^{13,14} of a two-dimensional self-interacting polymer. The number of hexagons visited by an SAW of length N is $H = N + 1 - N_2 - 2N_3$, where N_2 and N_3 are the numbers of hexagons visited twice and thrice by the SAW. Checking possible paths on the lattice shows that $H = N + 1 - I - I'$, where I is the number of self-contacts and I' the number of a certain type of next-nearest-neighbor contacts. The effects of I' are not believed to alter the universality class of the model^{13,14} and will be ignored. The weight $2^{-H} = 2^{-N-1+I}$ thus corresponds to the grand-canonical ensemble for polymers at chemical potential $\mu = -\log 2$ and with an attractive interaction energy $\beta U = -\log 2$ for each self-contact. We call a self-contact parallel (antiparallel) if, once a direction is defined along the polymer, the two sections of polymer in contact have the same (opposite) direction. For a long polymer, almost all self-contacts are antiparallel, as might be expected since parallel self-contacts are a boundary effect, in the weak sense that a closed polymer has none.

There are three phases of the θ' model for a two-dimensional self-interacting polymer. At high temperature, the statistical properties are those of the non-interacting SAW, and the mean radius of gyration is $R \sim N^{3/4}$. At low temperature, the polymer is in a collapsed phase with $R \sim N^{1/2}$. There is a tricritical point, called the θ -point, separating these two behaviors, with $R \sim N^{4/7}$. The importance of the θ -point for the plateau transition is that the weight 2^{-H} corresponds exactly to the θ -point on a honeycomb lattice. The chirality constraint will be shown to change the scaling and give the same universal properties as the solvable Manhattan lattice θ -point.

Now the diffusion at the critical energy can be obtained from (1.8). Considering for the moment only the SAW term in (1.8), the mean particle displacement after N steps is

$$\langle\langle R^2(N) \rangle\rangle = \sum_b P(a, b, N) (\mathbf{x}_b - \mathbf{x}_a)^2$$

$$= \sum_{\text{SAWs of length } N} \frac{R_{\text{SAW}}^2}{2^H} \sim \mu^N N^{\gamma-1+2\nu_\theta}. \quad (2.2)$$

Here we have introduced the standard polymer exponents γ and ν_θ , defined through

$$\sum_{\text{SAWs of length } N} \frac{1}{2^H} \sim \mu^N N^{\gamma-1} \\ \frac{\sum_{\text{SAWs of length } N} \frac{R_{\text{SAW}}^2}{2^H}}{\sum_{\text{SAWs of length } N} \frac{1}{2^H}} \sim N^{2\nu_\theta}. \quad (2.3)$$

For ordinary polymers (no chirality constraint) at θ , $\mu = 1$, $\gamma = \frac{8}{7}$, and $\nu_\theta = \frac{4}{7}$. The effect of the chirality constraint is clearly to reduce γ , since some polymers are forbidden: in fact we now show that $\gamma = \frac{6}{7}$ with the chirality constraint (μ and ν_θ are unchanged), so that $\langle\langle R^2(N) \rangle\rangle \propto N$ in (2.2) and motion is diffusive at the critical energy.

The critical properties of chiral polymers at θ are actually related in a very simple way to those of ordinary polymers at θ . As shown at the end of this section, the transfer matrix for L chiral polymers on a cylinder of finite circumference N hexagons has the same leading eigenvalue as the transfer matrix of $2L$ nonchiral polymers on the same cylinder. This means that the critical exponents for the chiral model can be deduced from the known values for the nonchiral model.

The “watermelon” exponents x_L ^{10,14} are defined from the correlation functions $G_{n,L}(a, b)$ of L mutually avoiding SAW’s from a to b at criticality: $G_{n,L}(a, b) \propto |a - b|^{-2x_L(n)}$. The natural generalization for the chiral case is that the L self-avoiding walks have no parallel self-contacts. Then the computation below of the transfer matrix at criticality ($\mu = 1$) on finite strips shows that the chiral exponents \tilde{x}_L are identical to the nonchiral exponents x_{2L} for twice as many connectors. The nonchiral values $x_L = (L^2 - 1)/12$ known from the Coulomb-gas technique¹⁰ then determine all the \tilde{x}_L .

Now we connect the watermelon exponents to physical properties such as γ and ν_θ . First, the size exponent $\nu_\theta = (2 - x_2)^{-1}$ is unchanged by the chirality constraint because it takes the same value for ring polymers as for linear polymers, and ring polymers are unaffected by the chirality constraint. The exponent γ is given by $\nu_\theta(d - 2\tilde{x}_1) = \nu_\theta(d - 2x_2) = \frac{6}{7}$. Note that the ring exponent α is¹⁴ also $\frac{6}{7}$ so the two terms of (1.8) scale with the same power of N , as required for consistency.

The diffusion result $\langle\langle R^2(N) \rangle\rangle \propto N$ might seem almost coincidental. However, it follows directly from the relationship $\tilde{x}_1 = x_2$ between the chiral exponent with one leg and the nonchiral exponent with two legs:

$$\gamma + 2\nu_\theta - 1 = \frac{4 - 2x_2}{2 - x_2} - 1 = 1. \quad (2.4)$$

The “mysterious cancellation of exponents”¹² which yields diffusion in the percolation picture is relatively

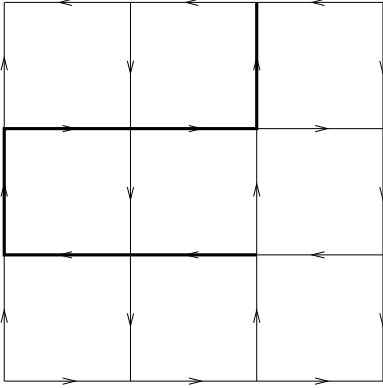


FIG. 2. A directed walk on the Manhattan lattice. Note that all allowed self-contacts on this lattice are antiparallel.

simple in the polymer picture, and does not depend on the specific value of x_2 .

The result $\tilde{x}_L = x_{2L}$ for chiral polymers is exactly the same as for polymers at θ on the Manhattan directed lattice (Fig. 2), which by construction has no parallel self-contacts¹⁷. Hence we learn that the detailed structure of the Manhattan lattice is in some sense irrelevant: it is the short-ranged constraint of no parallel self-contacts which determines the universality class. Another piece of information about polymers follows from the beautiful result of Cardy¹⁸ for the conductivity $\sigma_{xx} = \frac{\sqrt{3}e^2}{4h}$ at the critical energy. This fixes the lattice diffusion constant through the Einstein relation^{11,12}, and therefore predicts a value for the combination of prefactors in (2.2).

The chiral polymer model discussed here is just one point of a two-parameter family of models with antiparallel self-contacts weighted by some real number w and parallel self-contacts by some possibly different number v . Then $w = v$ gives ordinary two-dimensional self-interacting polymers, while $v = 0$ gives the chiral polymer ensemble. One expects a “coiled” polymer phase for $w = 0$ and $v \rightarrow \infty$, different from the conventional collapsed polymer phase. The full phase diagram of these models is an interesting topic for further study.

The remainder of this section establishes the connection $\tilde{x}_L = x_{2L}$ between the watermelon exponents of chiral polymers and those of nonchiral polymers, and can be skipped by nonspecialists. A powerful method to obtain properties of polymer models is by using conformal invariance to analyze the results of finite-size transfer matrix calculations^{19,20}. Since there are reviews of the technique^{20,21}, some minor details will be omitted.

The goal will be to find the transfer matrix for L polymers on a cylinder of circumference h hexagons. The scaling dimensions \tilde{x}_L can be derived from the finite-size correlation length $\xi_{L,h}$, which is determined by the largest eigenvalue $\lambda_{L,h}$ of the transfer matrix:

$$\xi_{L,h} = -\frac{1}{\log \lambda_{L,h}}. \quad (2.5)$$

The \tilde{x}_L are then estimated for successively larger cylin-

ders using

$$\tilde{x}_{L,h} = -\left(\frac{2}{\sqrt{3}}\right) \frac{h}{2\pi} \log \lambda_{L,h}. \quad (2.6)$$

The geometrical factor $\frac{2}{\sqrt{3}}$ comes from the hexagonal lattice dimensions and is 1 for a square lattice.

The transfer matrix acts on “configurations” of horizontal edges. A configuration consists of the state of all the horizontal edges, plus information on which oppositely directed edges are paired (originated from the same loop), plus information on which hexagons between horizontal edges have been passed on the left or right. The entries in the matrix sum over the different possible states of the vertical edges which can link two configurations. Each entry is weighted by a factor w for each hexagon passed on one side, v for each hexagon passed on both sides, and μ for each edge. For the critical point of chiral polymers, $w = \frac{1}{2}$, $v = 0$, and $\mu = 1$; setting $v = w = \frac{1}{2}$ gives the ordinary θ -point, while taking $w = v = 1$ and $\mu = \mu_c = (2 + \sqrt{2})^{-1}$ gives the critical point of noninteracting SAWs.

Note that parallel self-contacts can only occur for one polymer in the cylindrical geometry when the polymer winds around the cylinder. As a result the surface critical exponents, which follow from the transfer matrix on the strip (closed boundary conditions) rather than on the cylinder (periodic boundary conditions), are unmodified from the nonchiral case. Upon conformal mapping from the cylinder back to the plane, polymers which wrap around the cylinder become polymers which wrap around the origin of the plane, and closed boundary conditions correspond to a branch cut which polymers cannot cross. The equivalence of surface exponents to those of the nonchiral θ -point was previously obtained for the Manhattan lattice²².

Table I gives the estimated scaling dimensions \tilde{x}_1 and \tilde{x}_2 from cylinders of various sizes. The first few can be done by hand, while the larger matrices are done by computer. The leading eigenvalues are exactly the same as for those of twice as many nonchiral polymers. This connection is in retrospect not too surprising, since the condition of no parallel self-contacts for a polymer from A to B in the chiral case is exactly the condition that another polymer can be added from A to B in the nonchiral case. The subleading eigenvalues can differ, however, so there may not be a simple equivalence between states of L chiral polymers and $2L$ nonchiral polymers. The critical properties of the nonchiral model follow from Coulomb gas results for the $O(n)$ model¹⁰, so we have

$$x_L = \frac{L^2 - 1}{12}, \quad \tilde{x}_L = \frac{4L^2 - 1}{12}. \quad (2.7)$$

The chiral exponents \tilde{x}_L are the same as those of the θ -point on the Manhattan lattice²³. There are Monte Carlo results for another hexagonal lattice model believed to lie in the Manhattan universality class, the “smart kinetic growth SAW”²⁴, which are consistent with the above values.

h	$\tilde{x}_{1,h} = x_{2,h}$	$x_{\text{extrap.}}$	$\tilde{x}_{2,h} = x_{4,h}$	$x_{\text{extrap.}}$
2	0.254768			
3	0.259127	0.23788		
4	0.256212	0.24859	1.52861	1.2814
5	0.254221	0.24911	1.39654	1.26398
6	0.253007		1.34308	1.25603
7	0.25224		1.31513	
8			1.2984	
∞	$\frac{1}{4} = 0.25$		$\frac{5}{4} = 1.25$	

TABLE I. Results of transfer matrix calculations for one and two chiral polymers (identical to results for two and four nonchiral polymers), on cylinders of circumference h hexagons. The largest eigenvalue of the transfer matrix is related to $x_{L,h}$ through (2.6). The convergence to the predicted values $\tilde{x}_1 = \frac{1}{4}$ and $\tilde{x}_2 = \frac{5}{4}$ is seen to be quite rapid. The extrapolated values are obtained by using three consecutive values of x_h to fix the constants in $x_h = c_1 + c_2 h^{-c_3}$, then taking c_1 as an estimate of x_∞ .

III. THE CLASSICAL LOCALIZATION EXPONENT

When the particle energy E moves away from the critical energy, the trajectories become less extended and the mean distance from the origin after N time steps is reduced. In this section, we take the lattice disorder average in order to express $P(a, b, N)$, the probability that after N steps the particle has moved from a to b , as a weighted sum over linear and ring polymers. Simple properties of the weight function then yield an inequality connecting the localization exponent ν to polymer exponents γ and ν_θ .

As in the preceding section, we fix an open or closed curve on the lattice and ask what fraction of potential realizations make this curve the correct trajectory. The particle energy E is also varied in order to find the energy-integrated diffusion constant, and hence ν . The weight of a curve is determined by the numbers of hexagons touched by the curve to the left and right: the requirement for a path to be the correct trajectory is that all the hexagons to the right lie above the particle energy. The probability that a path is the particle trajectory is a function of the number of different hexagons visited by the path. The requirement is that all the hexagons to the immediate left have energies larger than the particle energy, while those to the immediate right have energies smaller than the particle energy. The H_L hexagons on the left must have higher energies than the H_R on the right, which is true for $(\frac{H_L+H_R}{H_L})^{-1}$ of potentials. Furthermore, the particle energy must lie in the window of width $\sim (H_L + H_R)^{-1}$ between the lowest potential on the left and the highest potential on the right. So the

weight of an allowed path P_{AB} is

$$W(P_{AB}) \propto \frac{1}{(H_L + H_R) \binom{H_L+H_R}{H_L}} \approx \frac{H_L! H_R!}{(H_L + H_R + 1)!}. \quad (3.1)$$

The same result is obtained by integrating the probability $(\frac{1+E}{2})^{H_L} (\frac{1-E}{2})^{H_R}$ over particle energy E to obtain a beta function.

Now we can again connect the expression (1.8) and the weight (3.1) to known properties of polymers. For fixed $H = H_L + H_R$, the weight is minimized if $H_L = H_R$, and using Stirling's approximation is then $W(H) \approx \frac{\sqrt{2\pi}}{2^H H^{1/2}}$. The probability to get from a to b after N steps thus satisfies

$$P(a, b, N) \geq \sum_{\substack{\text{SAPs through } a \text{ and } b, \\ l = \text{length of SAP,} \\ q = \text{steps from } a \text{ to } b}} \frac{\delta_{N \bmod l, q}}{2^H H^{1/2}} + \sum_{\substack{\text{SAWs of length } N \\ \text{from } a \text{ to } b \\ \text{no || self-contacts}}} \frac{1}{2^H H^{1/2}}, \quad (3.2)$$

up to a possible numerical constant. The typical number of hexagons H scales linearly in N to sufficient accuracy that $H^{1/2}$ can be replaced by $N^{1/2}$ (this is verified numerically by Monte Carlo simulations, and if false would require an unexpected multifractality at the θ -point). Summing over final positions b to find the mean squared displacement then gives

$$\langle\langle R^2(N) \rangle\rangle \geq N^{\gamma-1+2\nu_\theta-\frac{1}{2}}. \quad (3.3)$$

Then from equation (1.7) we obtain an inequality connecting the localization exponent ν for the plateau transition to polymer exponents ν_θ and γ :

$$1 - \frac{1}{2\nu} \geq \gamma + 2\nu_\theta - \frac{3}{2}. \quad (3.4)$$

For the chiral polymer model, the resulting prediction is $\nu \geq 1$, which is satisfied by the actual value $\nu = \frac{4}{3}$. The usual nonchiral polymer exponents at θ would predict $\nu \geq \frac{7}{3}$ (cf. section IV), so again it is seen that the chirality constraint is essential. The fact that the lower bound is not reached shows that even in the limit of long paths, the number of hexagons to the left and right of the path cannot be assumed equal in calculating the weight (3.1). At the critical energy (section II), hexagons to the left and right contribute equally and this difference is irrelevant, but away from the critical energy the difference affects the scaling.

The exact value $\nu = \frac{4}{3}$ is derived in the percolation picture⁴ from the equivalence of closed trajectories at energy E to percolation hulls with $p - p_c \propto E - E_0$, where p_c is the critical probability for percolation and E_0 is the critical energy. Such percolation hulls²⁵ have

average size $\xi \sim (p - p_c)^{-\frac{4}{3}}$. We remark in passing that the value $\nu = \frac{4}{3}$ can be understood in the polymer context from the fact the crossover exponent of the tricritical θ -point is $\phi = \frac{3}{7}$ (this value was first obtained using the connection to percolation¹⁴): then $N^{-\phi} \sim (p - p_c)$ and $\xi \sim (p - p_c)^{-\nu\theta/\phi} = (p - p_c)^{-\frac{4}{3}}$. The reasons for stressing the inequality (3.4) here rather than the exact result are that the inequality follows immediately from the classical path weight on polymers, and that hence a similar inequality is expected to apply for the quantum transition, as discussed in section IV.

The main result of this section is that the exact path weight induced by averaging over disorder and particle energy can be calculated for the classical lattice model. This weight yields the inequality (3.4) connecting statistics of chiral polymers to the critical exponent ν of the classical plateau transition. The focus of the next section will be whether a similar relationship to polymers exists for the quantum plateau transition.

IV. THE QUANTUM TRANSITION

The first step toward the quantum problem is explaining why quantum effects can be described within the polymer formulation at all. For fixed disorder, different paths W_{AB}^i from A to B contribute to the amplitude, and the probability P_{AB} to get from A to B includes both diagonal terms $|W_{AB}^i|^2$ and cross terms. We start by considering two paths which do not cross. Then the situation is similar to the two-slit experiment of Fig. 3: a random Aharonov-Bohm flux Φ between the two slits gives the two paths a relative phase $e^{i\Phi}$ which shows up in cross terms. The cross terms can be of the same magnitude as the diagonal terms. However, when Φ is averaged, the cross terms disappear because of their random phase, leaving the diagonal terms. An uncertainty remains in the problem (the particle can go through either slit) but the interference has disappeared after flux-averaging. In the QHE problem, two paths separated by more than a disorder correlation length λ_D will get a random phase, and after disorder averaging only diagonal terms will contribute to P_{AB} . The remaining question is what occurs for intersecting paths; this is known to be the case of interest for the quantum effects causing weak localization.

Weak localization arises from constructive interference between paths which trace the same loop in opposite directions. The famous negative magnetoresistance arises because a magnetic field generates a phase between the two directions around the loop and weakens the interference. In the strong-magnetic-field limit implied by the semiclassical picture of the plateau transition, only one of two directions around a loop can have appreciable amplitude in a fixed disorder realization. Since it is essential for significant interference that both paths have appreciable amplitude in the same disorder realization, the quantum corrections of the type causing weak local-

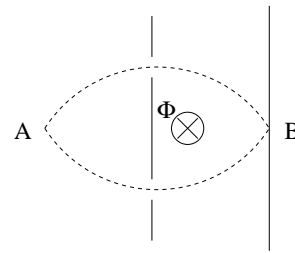


FIG. 3. A two-slit experiment to illustrate interference between two paths from A to B in the presence of Aharonov-Bohm flux Φ .

ization are absent in the strong-field limit. This lack of interference suggests that the disorder-induced vanishing of cross terms is not restricted to nonintersecting paths. If the cross terms do vanish, then in the discretized model where λ_D is effectively zero, P_{AB} must be a sum over (not necessarily self-avoiding) paths with some positive weight, the “quantum path weight” (QPW). The conclusion of the above argument is that the universal large-length-scale properties of the plateau transition may be related to those of some classical generalized polymer model (i.e., a sum over paths with positive weights), in similar fashion to the relationships found in sections II and III between the classical percolation limit and the chiral polymer model.

The remaining step is to determine which universal class of classical polymers includes the QPW, whose details are unknown. It is not certain that the QPW corresponds to any physically interesting class of polymers, but it seems worthwhile to identify possibilities, since exact results have been obtained for many two-dimensional polymer models by Coulomb gas and CFT techniques. In the following, we discuss how the classical path weight should be modified by the incorporation of quantum effects. Then two classes of polymers are discussed which may be relevant to the quantum case.

The QPW should give nearly the weight of (3.1) to paths which are classically allowed or include a small number of quantum tunneling events, but should not allow of order N tunneling events for an N -step path since then the motion is simply diffusive even away from the critical energy. The reason why quantum corrections act to increase ν can be understood heuristically as follows: a percolation hull has many “fjords” where a tunneling event can reduce the number of steps required to travel a given distance (Fig. 4). From numerical studies of the transition^{6,7}, the correct quantum description should have a localization length exponent $\nu = 2.35 \pm 0.05$ and should also show diffusion at the critical energy. In the remainder, possible weights on chiral and nonchiral polymers at θ are discussed in the context of these two restrictions. The advantage of the chiral model is that diffusion emerges naturally as in section II, while for the nonchiral model, the value $\nu = \frac{7}{3}$ (which has attracted attention as the simplest rational consistent with numer-

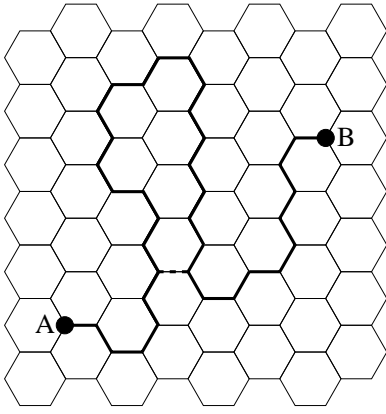


FIG. 4. An example of how one tunneling event (the dashed line) can reduce the length required for the electron to reach B from A , by truncating a fjord.

ics) appears somewhat surprisingly from exponents of the polymer ensemble.

In section III it was shown that the value $\nu = \frac{4}{3}$ in the classical limit depends on the fact that paths with more hexagons to the left H_L than to the right H_R , or vice versa, have larger classical weight (3.1) than those with $H_L = H_R$. However, paths with a large difference between H_L and H_R are highly convoluted and on average shorter than those of the same length with $H_L = H_R$. One effect of quantum mechanics is to shift some probability from the convoluted paths to the straighter ones (if the particle trajectories continue to have well-defined energy E , then the total probability should be conserved for all paths at energy E). Then the averaged displacement will increase, increasing the predicted exponent ν . In order to explain the numerical result $\nu \approx \frac{7}{3}$, the mean squared displacement $\langle\langle R^2(N) \rangle\rangle$ must increase from $N^{5/8}$ to $N^{11/14}$. We have been unable to answer analytically the question of whether any simple shifting of probability at constant energy is sufficient, and are currently carrying out a Monte Carlo study.

A more interesting but admittedly speculative connection is to *nonchiral* polymers at θ . The physical expectation that quantum mechanics should allow some unfavorable steps (but fewer than $\sim N$) matches the fact that a typical polymer in the nonchiral ensemble has some parallel self-contacts, but fewer than of order N . A simple argument that the number of parallel self-contacts is subextensive ($< N$) is that a ring polymer has no parallel self-contacts, so that parallel self-contacts are in some sense a boundary property.

Since parallel self-contacts correspond to hexagons passed on both sides, the classical path weight (3.1) is undefined when such hexagons are present. If such (relatively rare) hexagons do not modify the weight qualitatively, then the inequality (3.4) connecting the localization exponent ν to nonchiral polymer exponents predicts

$$1 - \frac{1}{2\nu} \geq \gamma + 2\nu_\theta - \frac{3}{2} = \frac{11}{14}, \quad (4.1)$$

or $\nu \geq \frac{7}{3}$. Hence the number $\frac{7}{3}$ comes out of the critical properties of a polymer ensemble closely related to the polymer ensemble describing the classical plateau transition (the conditions for the lower bound to be realized are discussed below). Note that the previous appearance of $\frac{7}{3}$ in a semiclassical average over a single percolation trajectory²⁶ does not (at least naively) access the critical point, when the electron is delocalized over multiple trajectories.

The chief problem of the nonchiral ensemble is in explaining diffusion at the critical energy: obtaining diffusion in section II depended on the value $\gamma = \frac{6}{7}$ for chiral polymers, while the corresponding value for nonchiral polymers $\gamma = \frac{8}{7}$ would naively give superdiffusive behavior. However, recall that in the quantum case any eigenstate has a finite extent in the direction of the potential gradient, so that the “trajectory energy” (in the classical case, the value of the classical potential at the guiding center) has some uncertainty, even though the full energy of the eigenstate is constant. Hence eigenstates at the critical energy do not correspond only to paths at the mean of the potential, with trajectory energy E_0 , but integrate over some window in trajectory energy, so that the superdiffusive behavior is not necessarily inconsistent. However, this picture means that the critical conductivity is not an obvious universal property of the polymer problem.

This situation is familiar from the Liouvillian approach to the transition^{16,27}, where the transition is mapped onto a different problem which contains the exponent ν but not the critical conductivity. Now consider again the disorder- and energy-averaged displacement $\langle\langle R^2(N) \rangle\rangle \propto N^{1-\frac{1}{2\nu}}$. The lower bound in the inequality $\nu \geq \frac{7}{3}$ is attained if the numbers of hexagons H_R and H_L of a typical path are nearly equal. So for the nonchiral ensemble to be the correct one and $\nu = \frac{7}{3}$ to be the exact value, quantum mechanics must have two nontrivial effects beyond allowing some classically unfavorable tunneling events: it must induce an uncertainty in the “trajectory energy” of the previous paragraph, and cause typical paths to have fewer fjords than in the classical case (so that $H_L \approx H_R$). While the connection to the nonchiral ensemble is, again, speculative, it is noteworthy that the required assumptions coincide to some degree with the heuristic expectation for what quantum effects should do. It seems that a serious numerical calculation of the QPW in a specific model for tunneling events is required to justify the analogy further.

To summarize, the bulk of this section conjectured a relationship between the quantum plateau transition and the statistics of two-dimensional polymers. In closing we discuss briefly connections between this picture and conformal field theory (CFT) approaches to the transition. The low-temperature $O(n)$ phase also appears in a large- N expansion of the disorder-averaged Liouvillian theory, which is formally similar to a partially supersymmetrized $O(N)$ model, with $N \rightarrow 1$ the physical limit²⁷. The evi-

dence from two energy-integrated approaches is that ν is associated with the central charge $c = 0$ low-temperature $O(n \rightarrow 1)$ theory, while the critical conductivity and other energy-specific properties may require a more complicated $c = -2$ theory³. Finally, a recent study²⁸ of the critical point of Dirac fermions in a random vector potential found a $c = -2$ dense polymer problem hidden in the critical theory for several different types of disorder. Since upon adding additional disorder (random mass and chemical potential) this critical point flows to the plateau transition fixed point²⁹, the appearance of polymer subalgebras may be generic to this class of random critical points.

The author wishes to thank H. Saleur and S. Girvin for helpful suggestions.

-
- ¹ R. B. Laughlin, Phys. Rev. B **23**, 5632 (1981).
² A. M. M. Pruisken, Nucl. Phys. B **235**, 227 (1984).
³ M. Zirnbauer, J. Math. Phys. **38**, 2007 (1997).
⁴ S. Trugman, Phys. Rev. B **27**, 7539 (1983).
⁵ I. A. Gruzberg, A. W. W. Ludwig, and N. Read, Phys. Rev. Lett. **82**, 4524 (1999).
⁶ B. Huckestein, Rev. Mod. Phys. **67**, 357 (1995).
⁷ J. T. Chalker and P. D. Coddington, J. Phys. C **21** 2665 (1988).
⁸ S. Das Sarma, in *Perspectives in Quantum Hall Effects*, ed. S. Das Sarma and A. Pinczuk (Wiley, New York, 1997).
⁹ P. G. de Gennes, Phys. Lett. **A38**, 339 (1972).
¹⁰ B. Nienhuis, Phys. Rev. Lett. **49**, 1063 (1982); B. Nienhuis, in *Phase Transitions and Critical Phenomena*, ed. C. Domb and J. L. Lebowitz (Academic, London, 1986), vol. 11.
¹¹ F. Evers, Phys. Rev. E **55**, 2321 (1997).
¹² V. Gurarie and A. Zee, cond-mat/0008163 (2000).
¹³ A. Coniglio *et al.*, Phys. Rev. B **35**, 3617 (1987).
¹⁴ B. Duplantier and H. Saleur, Phys. Rev. Lett. **59**, 539 (1987).
¹⁵ H. P. Wei, D. C. Tsui, M. A. Paalanen and A. M. M. Pruisken, Phys. Rev. Lett. **61**, 1294 (1988); H. P. Wei, S. Y. Lin, D. C. Tsui, and A. M. M. Pruisken, Phys. Rev. B **45**, 3926 (1992).
¹⁶ J. Sinova, V. Meden, and S. M. Girvin, Phys. Rev. B **62**, 2008 (2000).
¹⁷ R. M. Bradley, Phys. Rev. A **41**, 914 (1990).
¹⁸ J. Cardy, Phys. Rev. Lett. **84**, 3507 (2000).
¹⁹ B. Derrida, J. Phys. A **14**, L5 (1981).
²⁰ H. Saleur, J. Phys. A **20**, 455 (1987).
²¹ C. Vanderzande, *Lattice Models of Polymers* (Cambridge, 1998).
²² S. L. M. de Queiroz and J. M. Yeomans, J. Phys. A **24**, L933 (1991).
²³ T. Prellberg and A. Owczarek, J. Phys. A **27**, 1811 (1994).
²⁴ D. Bennett-Wood, A. L. Owczarek, and T. Prellberg, Physica A **206**, 283 (1994).
²⁵ M. den Nijs, J. Phys. A **12**, 1857 (1979).

- ²⁶ G. V. Mil'nikov and I. M. Sokolov, JETP Lett. **48**, 536 (1988).
²⁷ J. E. Moore, A. Zee, and J. Sinova, cond-mat/0012341 (2000).
²⁸ M. J. Bhaseen, J.-S. Caux, I. I. Kogan, and A. M. Tsvelik, cond-mat/00012240 (2000).
²⁹ A. W. W. Ludwig, M. P. A. Fisher, R. Shankar, and G. Grinstein, Phys. Rev. B **50** 7526 (1994).